Morphological Changes and Fusogenic Activity of Influenza Virus Hemagglutinin

Tong Shangguan,* David P. Siegel,# James D. Lear,§ Paul H. Axelsen,¶ Dennis Alford,* and Joe Bentz*

*Department of Bioscience and Biotechnology, Drexel University, Philadelphia, Pennsylvania 19104; #Procter and Gamble Co., Miami Valley Labs, Cincinnati, Ohio 45239; §Department of Biochemistry and Biophysics, University of Pennsylvania, Philadelphia, Pennsylvania 19104; and ¶Department of Pharmacology and the Johnson Foundation for Molecular Biophysics, University of Pennsylvania, Philadelphia, Pennsylvania 19104 USA

ABSTRACT The kinetics of low-pH induced fusion of influenza virus with liposomes have been compared to changes in the morphology of influenza hemagglutinin (HA). At pH 4.9 and 30°C, the fusion of influenza A/PR/8/34 virus with ganglioside-bearing liposomes was complete within 6 min. Virus preincubated at pH 4.9 and 30°C in the absence of liposomes for 2 or 10 min retained most of its fusion activity. However, fusion activity was dramatically reduced after 30 min, and virtually abolished after a 60-min preincubation. Cryo-electron microscopy showed that the hemagglutinin spikes of virions exposed to pH 4.9 at 30°C for 10 min underwent no major morphological changes. After 30 min, however, the spike morphology changed dramatically, and further changes occurred for up to 60 min after exposure to low pH. Because the morphological changes occur at a rate corresponding to the loss of fusion activity, and because these changes are much slower than the rate at which fusion occurs, we conclude that the morphologically altered HA is inactive with respect to fusion-promoting activity. Molecular modeling studies indicate that the formation of an extended coiled coil within the HA trimer, as proposed for HA at low pH, requires a major conformational change in HA, and that the morphological changes we observe are consistent with the formation of an extended coiled coil. These results imply that the crystallographically determined low-pH form of HA does occur in the intact virus, but that this form is not a precursor of viral fusion. It is speculated that the motion to the low-pH form may be responsible for the membrane destabilization leading to fusion.

INTRODUCTION

The hemagglutinin (HA) of influenza is the major glycoprotein component of the viral envelope. It has a dual function in mediating attachment of the virus to the target cell and fusion of the viral envelope membrane with target cell membranes. HA is homotrimeric and is composed of two polypeptide segments, designated HA1 and HA2. The HA1 segments form sialic acid-binding sites and mediate HA attachment to the host cell surface. The HA2 segment forms the membrane-spanning anchor (Wiley and Skehel, 1987), and its amino-terminal region appears to be directly involved in the fusion reaction mechanism (Gething et al., 1986). Fusion appears to require more than one HA trimer at the fusion site, and it is likely that the HA molecules involved in cell surface attachment are not involved in fusion (Ellens et al., 1990; Bentz, 1992; Alford et al., 1994).

In the normal course of viral infection, virus bound to the cell surface is taken up into endosomes and exposed to relatively low pH. The pH change triggers fusion between the viral envelope and the endosomal membrane, as well as conformational changes in HA, which lead to increased exposure of the amino terminus (Skehel et al., 1982; White and Wilson, 1987; Ruigrok et al., 1988; Godley et al., 1992). Crystallographic studies of the HA ectodomain at neutral pH (BHA, Wilson et al., 1981) and a portion of HA prepared by treating BHA with proteolysis at low pH (TBHA2, residues 38–175 of HA2 and 1–27 of HA1 held together by the disulfide bond; Bullough et al., 1994) have yielded considerable insight into the nature of these pH-triggered conformational changes. The most remarkable finding of these studies is that the triple-stranded α-helical coiled coil of BHA, involving residues 82–125, is extended proximally in TBHA2 to involve residues 38–175, incorporating portions of BHA that had been random coil (residues 54–81) and α-helix (residues 38–53). These findings were essentially as predicted by Carr and Kim (1993) and later supported by the studies of Chen et al. (1995).

As a consequence of this rearrangement, the N-terminus of HA2 is thrust ~100 Å toward the target membrane, so that direct interaction between the N-terminus of HA2 and the target membrane is possible. However, it is not clear that this interaction is essential for fusion (Bentz et al., 1990; Stegmann et al., 1990), and the behavior of TBHA2 may not reflect that of the intact HA, because it represents only ~30% of the native protein. In any case, the crystallographic findings, considered together with the studies of Carr and Kim (1993) and Chen et al. (1995), suggest that the extended coiled-coil structure is the most stable, equilibrium structure of HA at low pH.

The formation of extended coiled-coil structures may be involved in fusion-related processes in viruses other than influenza. For example, Wild et al. (1994) identified a putative

Received for publication 23 June 1997 and in final form 14 October 1997.

Address reprint requests to Dr. Joseph Bentz, Department of Bioscience and Technology, Drexel University, 32nd & Chestnut Sts., Philadelphia, PA 19104-2875. Tel.: 215-895-2624. Fax: 215-895-1273; E-mail: bentzj@duvm.ocs.drexel.edu.

Dr. Alford's present address is Center for Blood Research, Boston, MA 02115.

Dr. Shangguan's present address is The Liposome Company, Princeton, NJ 08540.

© 1998 by the Biophysical Society

0006-3495/98/01/54/09 $2.00

coiled-coil region on the envelope protein gp41 of human immunodeficiency virus (HIV). Peptides corresponding to this region formed α-helices below 40°C, blocked HIV infection, and inhibited syncytium formation. The authors speculated that these peptides bind to the putative coiled-coil region of gp41 and block the interaction between gp120 and gp41. These sequences within gp41 form coiled coils (Chan et al., 1997; Weissenhorn et al., 1997), but whether the added peptides bind to gp120/41 is yet to be verified.

It remains to be determined how (and whether) these structural features are involved with HA-mediated membrane fusion, because there has been no direct correlation between low-pH induced conformations of HA and its "fusogenicity." It is known that influenza virions rapidly lose their ability to fuse with target membranes if they are incubated at low pH in the absence of target membranes (White et al., 1982; Sato et al., 1983; Stegmann et al., 1989; Puri et al., 1990; Nir et al., 1993). This implies that the equilibrium conformation of HA at low pH form is not fusogenic. Conversely, Puri et al. (1990) and Stegmann et al. (1990) showed that incubation of isolated virions (A/Japan/305/57 strain) at low pH resulted in no substantial morphological change in HA, yet they were still able to undergo fusion.

In this work we compare the kinetics of low-pH induced fusion of influenza virus with liposomes to changes in the morphology of influenza HA. Our results suggest that forms of HA with altered morphology are consistent with formation of the extended coiled-coil structure characterized crystallographically at low pH and that these forms are not fusogenic. Preliminary data from this work have been presented (Shangguan et al., 1996b).

MATERIALS AND METHODS

Materials

Dioleoylphosphatidylcholine (DOPC) was purchased from Avanti Polar Lipids (Alabaster, AL). Ganglioside G_{d1a} (G_{d1a}); bromelain; ultrol grade HEPES, tetrasodium salt; and octaethylene glycol monododecyl ether (C12E8) were purchased from Calbiochem (La Jolla, CA). *N'*-[[4-[7-(diethylamino)-4-methylcoumarin-3-yl]phenyl]-*N*-methylthioureidyl] phosphatidylcholine (CPT-PC) and [[[4-[[4-(dimethylamino)phenyl]azo] phenyl]sulfonyl]methylamino]phosphatidylcholine (DABS-PC) were generous gifts from Dr. John R. Silvius (McGill University, Montréal, Québec, Canada). The influenza A/PR/8/34 (H1N1) (catalog no. VR-95) inoculum was purchased from the American Type Culture Collection (ATCC) (Rockville, MD), thawed, subaliquoted, and stored at −80°C. Ten-day-old fertilized eggs were purchased from SPAFAS (Norwich, CT).

Virus purification

Influenza A/PR/8/34 (H1N1) was grown in fertilized chicken eggs and purified as described before (Shangguan et al., 1996a). The purified virus was collected from the 20%/40% sucrose interface, assayed for protein, quickly frozen, and stored at −80°C.

The viral phospholipid-protein ratio was determined as described (Shangguan et al., 1996a). The phosphate content was determined according to the method of Bartlett (1959). The phospholipid-protein ratio of PR/8 virus is 0.322 μmol/mg.

Liposome preparation

DOPC liposomes were prepared in 10 mM HEPES buffer saline (HBS) by reverse-phase evaporation procedures (Szoka and Papahadjopoulos, 1978) and extruded 5–10 times through 0.1-μm polycarbonate membrane filter (Poretics Corp., Livermore, CA). The liposomes were composed of 90 mol% DOPC, 10 mol% G_{D1a}, 0.6 mol% CPT-PC, and 0.6 mol% DABS-PC. The lipid concentration of the liposomes was determined by phosphate assay (Bartlett, 1959) and corrected for the 10 mol% G_{D1a}.

Fluorescence lipid mixing assay

Lipid mixing between unlabeled influenza PR/8 virus and CPT/DABS-labeled liposomes was measured in 10 mM HBS buffer by the resonance energy transfer (RET) assay (Silvius et al., 1987). This RET pair is less susceptible to protein conformational changes than other RET pairs tested (Alford et al., 1994; Shangguan et al., 1996a). CPT fluorescence was recorded on a PTI Alphascan fluorometer (South Brunswick, NJ) in a thermostatted cuvette with continuous stirring. The excitation and emission wavelengths were 395 and 477 nm, respectively. For the inactivation assay, 80 μl virus was incubated at pH 4.9, 30°C, for the designated period of time and injected into a cuvette containing 1.92 ml 10 mM HEPES buffer (pH 7.5) and liposomes. The final concentration was 10 μM viral phospholipid and 10 μM liposomal lipid. This fluorescence level was set as 0% lipid mixing. Lipid mixing was initiated after 50 s by injecting 20 μl 1.67 M acetic acid/acetate solution to reach pH 4.9. The fluorescence level at infinite probe dilution obtained by $C_{12}E_8$ (0.75 mM) lysis was considered as 100% lipid mixing.

BHA purification

BHA was purified as described (Brand and Skehel, 1972; Doms et al., 1985) with small modifications. Briefly, virus stock was quickly thawed, diluted with 10 mM HBS buffer, and pelleted at 100,000 × *g* for 1 h to remove sucrose. Virus (2 mg/ml) was resuspended in 10 mM HBS buffer containing EDTA (1 mM), bromelain (1 mg/ml), and 2-mercaptoethanol (0.05 mM) and incubated at 25°C overnight. After digestion, the mixture was centrifuged at 100,000 × *g* for 1 h to pellet viral cores. The supernatant was loaded on a ricin-agarose column (Sigma, St. Louis, MO). After extensive washing with 10 mM HBS buffer, BHA was eluted with 0.2 M galactose in HBS. The peak fractions were pooled and dialyzed extensively against 10 mM HBS buffer to remove galactose. The purified BHA was stored at 4°C. On sodium dodecyl sulfate polyacrylamide gel electrophoresis (SDS-PAGE), BHA appeared as a single band of M_r = 60,000 MW (data not shown).

Circular dichroism measurements

The measurements were made at 30°C in 1-cm quartz cells, with an Aviv Model 62DS instrument. Spectra were recorded with a 1-s time constant and 1-nm wavelength steps between 275 and 190 nm. After solvent baseline determination, 200 μl of purified BHA stock solution (0.134 mg protein/ml) in 10 mM HBS buffer was added to 3 ml of 10 mM sodium phosphate buffer (pH 7.0), and the spectrum was remeasured. Useful data could be obtained only down to 205 nm because of excessive UV absorption. The CD signal at 222 nm (~ −10 mdeg) was used to monitor conformational changes with time after acidification. The instrument time constant was reset from 1 to 5 s, and ellipticity measurements were made at a constant 222 nm over 10-s intervals. After ~10 min (to assess baseline drift), the solution was acidified by the addition of 20 μl 1 M phosphoric acid predetermined to give a final pH of 4.3, the cuvette contents were stirred, and measurements continued after 100 s (the time taken to carry out the acidification). After ~66 min, another 20-μl aliquot of phosphoric acid was added, which brought the pH down to 2.8 (measured after the experiment was done), and the kinetics measurement continued for another 10 min.

Cryo-transmission electron microscopy

Cryo-TEM specimens were prepared in a modified form (Siegel et al., 1994) of the controlled environment vitrification system (Bellare et al., 1988). Aliquots of virus were preincubated at 30°C, pH 7.4, for several minutes. Then either specimens were made directly, or equal volumes of virus suspension and low pH buffer (120 mM NaCl, 50 mM sodium acetate, 0.1 mM EDTA) were mixed and then incubated at 30°C for the indicated time periods. The pH of the acetate buffer was preadjusted to yield a final pH of 4.90 ± 0.02 in the mixture. At the indicated time points, 5-μl samples were withdrawn with a micropipette, applied to the TEM grid at room temperature, and blotted with a strip of filter paper to form a thin film. The 300-mesh copper TEM grids coated with a lacy carbon substrate are supplied by Ted Pella, Inc. (Redding, CA). The grid was then vitrified by plunging into liquid ethane and stored under liquid nitrogen. The time required to form and vitrify the TEM specimen at room temperature (22°C) was ~30 s. The final concentrations of virus in the specimens were between 0.1 and 0.3 mg viral protein/ml.

Specimens were mounted in a Gatan 626 cold stage (Gatan, Inc., Warrendale, PA). They were examined at ~ −170°C in a Philips CM12 TEM, operating at 100 kV. Images were obtained by using low-dose procedures, and no electron damage or devitrification was apparent in images used for morphological comparisons. The images were obtained on Kodak SO-163 film (Eastman Kodak Co., Rochester, NY) and were developed for 12 min in undiluted Kodak D-19 developer.

The focal settings of the cryo-TEM images in Fig. 2 were determined from the optical diffraction patterns of the corresponding negatives. They are −7, −8.2, −6.7, −5.2, and −3.7 μm for Fig. 2, *A*, *B*, *C*, *D*, and *E*, respectively. The first zero in the contrast transfer functions under these conditions was measured as 5.1, 5.5, 5.0, 4.4, and 3.5 nm, respectively. These conditions were chosen by eye so as to maximize the contrast of distinct HA trimer spikes. The first zeros in the contrast functions are at positions appropriate for this choice.

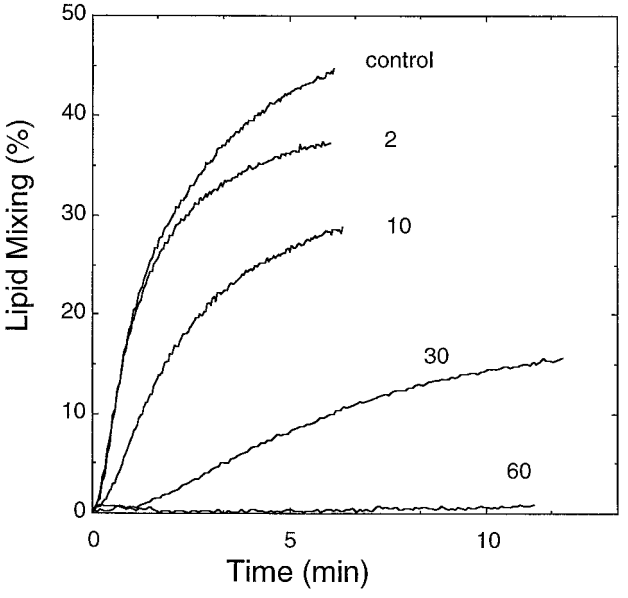

FIGURE 1 Inactivation of influenza PR/8 virus at 30°C. Unlabeled virus was incubated alone at 30°C, pH 4.9, for the indicated time in minutes shown next to each curve. At the end of each incubation period, virus was injected into cuvettes containing CPT/DABS labeled DOPC/G_{D1a} (90:10) liposomes at neutral pH. Lipid mixing was initiated after 50 s by acidification. Lipid mixing kinetics is shown as a function of inactivation time in minutes.

RESULTS

All experiments were performed at 30°C with influenza A PR/8/34, because this strain at this temperature exhibits favorable lipid mixing and viral inactivation kinetics (Shangguan, 1995). The HAs of PR/8/34 and the X-31 strain examined by Bullough et al. (1994) are highly homologous, but the latter inactivates too rapidly at or near 37°C (Stegmann et al., 1990) for these studies. Fig. 1 shows the mixing of lipid from unlabeled virus with DOPC/GD1a (90:10) liposomes labeled with 0.6 mol% of CPT-PC and DABS-PC. Lipid mixing leads to dilution of the labels into the viral envelope lipid and dequenching of CPT fluorescence. The inactivation kinetics for the virus were obtained by incubating virions at pH 4.9 and 30°C for the time periods indicated in minutes next to each curve and then adding them to liposomes at pH 7.4. The measurements are referenced to the time the liposome-virus mixture was acidified to pH 4.9. For a 0-min incubation, lipid mixing was complete in ~6 min. Incubation for 2 min was also complete in ~6 min. There was a 30–40% decrease in the rate of lipid mixing after a 10-min incubation, and the virus was completely inactive after a 60-min incubation at low pH.

To correlate these rates of fusion/inactivation with a conformational change in the HA of an intact virus, we used cryo-TEM to follow changes in the morphology of the virus surface spike layer as a function of incubation time at low pH. It has been shown that drastic conformational changes do occur in viral HA spikes and are visible via cryo-TEM (Puri et al., 1990; Stegmann et al., 1990). Fig. 2 *A* shows cryo-TEM micrographs of virions incubated at pH 7.4, without acidification. The appearance of the virions is the same as in previous cryo-TEM studies of PR/8 strain (Fujiyoshi et al., 1994; Alford et al., 1994) and other strains of influenza virus obtained under similar conditions (Booy et al., 1985; Stegmann et al., 1987; Ruigrok and Hewat, 1991; Puri et al., 1990; Ruigrok et al., 1992). Note that the HA trimer spikes on the surface of the virions are distinct and well defined.

Fig. 2 *B* shows virions incubated for 2 min at pH 4.9. The spikes on the virions are still distinct and well defined, as in Fig. 2 *A*. This micrograph was obtained slightly farther underfocus than the one in Fig. 2 *A*; hence the spikes appear slightly more distinct. In Fig. 2 *C* the virions had been incubated for 10 min at pH 4.9, and the spikes still appear as those at pH 7.4 (Fig. 2 *A*). After longer incubations, the HA spikes begin to appear disordered and less distinct, with less contrast in the parts of the spike closest to the viral membrane. In Fig. 2, *D* and *E*, the virions had been incubated for 68 min at pH 4.9, and all but one of the virions have disordered spikes. These changes are similar to those noted previously in the X-31 and X-47 strains of influenza virus incubated for extended times at pH 5 and 37°C (Stegmann et al., 1987; Puri et al., 1990). In Fig. 2 *D* a single virion (*arrowhead*) still resembles virions at pH 7.4. This demonstrates that the focus conditions used are appropriate for detecting gross changes in the conformation of the HA trimers. Only two such virions were found among ~1300 virions in images obtained after 60–68-min incubations. Similar results were obtained using preparations of influ-

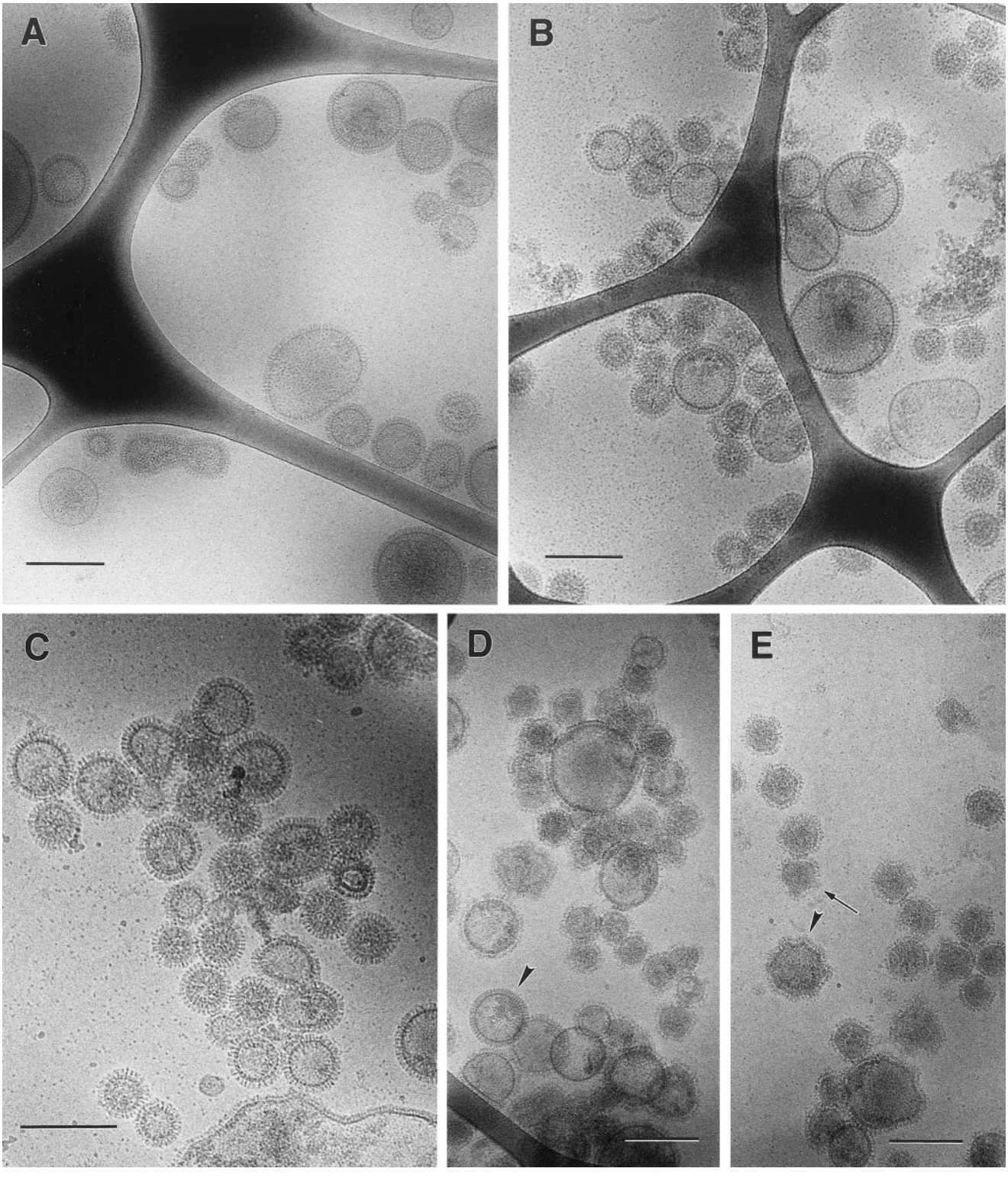

FIGURE 2 Cryo-TEM of influenza PR/8 virions at 30°C. (*A*) Influenza PR/8 virus at pH 7.4. (*B*) Influenza virus incubated for 2 min at pH 4.9. Note that the spikes on the virions are still distinct and well-defined, as in *A*. (*C*) Virions incubated for 10 min at pH 4.9. Spikes are still well defined and distinct. (*D*) Virions incubated for 68 min at pH 4.9. Note that the spikes on the virions have become disorganized and are no longer well defined or distinct. This field was chosen because it contains a rare sample of a virion with organized spikes like those in *A* (*arrowhead*), which shows that the focus conditions were appropriate for detecting spikes. (*E*) Another example of virions incubated at pH 4.9 for 68 min. Many of the virions incubated under these conditions had blebs and discontinuities visible on their surfaces. Examples of such features are shown in the membrane of small (*arrow*) and large (*arrowhead*) virions. Scale bars = 200 nm in all figures.

enza virions that were never frozen, but were examined within 2 days of isolation (data not shown).

We also examined specimens incubated for 30 min at pH 4.9, although we obtained a smaller number of images for these conditions. Examples are shown in Fig. 3. After 30 min, most of the virions had disorganized spike layers (Fig. 3 *A*), resembling the virions incubated for 68 min. However, there were more examples of virions with organized spike layers (*arrowheads* in Fig. 3 *B*) than in samples incubated for 68 min, where they were extremely rare (Fig. 2 *D*). Our data are insufficient to determine whether the spike layers disorganize in a cooperative fashion (i.e., whether all of the spikes on an individual virion change conformation more or less simultaneously).

Fig. 4 shows higher magnification images of virions to emphasize the change in spike morphology that is induced by prolonged incubation at low pH. Fig. 4 *A* shows virions incubated at pH 7.4 and 30°. Fig. 4, *B* and *C*, shows virions incubated at pH 4.9 and 30° for 10 min and 68 min, respectively. Fig. 4, *B* and *C*, are blown-up portions of Fig. 2, *C* and *D*, respectively. Fig. 4 *A* is taken from a different negative than Fig. 2 *A*, which was obtained with defocus conditons more similar to Fig. 4, *B* and *C*.

Figs. 2, *B–D*, and 3 show that influenza virions tended to aggregate at low pH. This was especially true for the smaller particles (i.e., diameters of $\sim$0.13 μm or less), which were the most numerous. This is significant with respect to photoaffinity labeling results of Weber et al. (1994), who found that the N-termini of HA2 were embedded into viral envelopes upon inactivation. Based on the claim that light-scattering data did not indicate virus aggregation, they claimed that the N-terminal regions must insert into their own envelope, as has been suggested previously (Ruigrok et al., 1986) and more recently (Weissenhorn et al., 1997). Because the virions do aggregate, it has yet to be shown whether the N-terminus of HA2 can insert into its own envelope rather than simply inserting into the envelope of an adjacent virion.

There were two other types of changes induced by low pH incubation. First, with increasing incubation time, virions developed discontinuities (Fig. 2 *E*, *arrowhead*) or bleblike structures (*arrow*) in their membranes. Similar membrane features were observed previously with strain X-31, incubated for 30 min at pH 5 and room temperature (Ruigrok et al., 1992). Discontinuities first appeared in significant numbers after 10 min at pH 4.9 and were very common after 60 min. Some of the virions became quite irregular after 60–68 min, with blebs around their entire periphery. Second, we consistently found a small fraction of virions at pH 7.4 to have elongated, nonspherical shapes. However, very few such structures were observed after 2 min at pH 4.9. This was especially true in the case of long tubular virions, which were essentially absent after incubations of more than 2 min. Similar behavior has been observed previously in various strains of

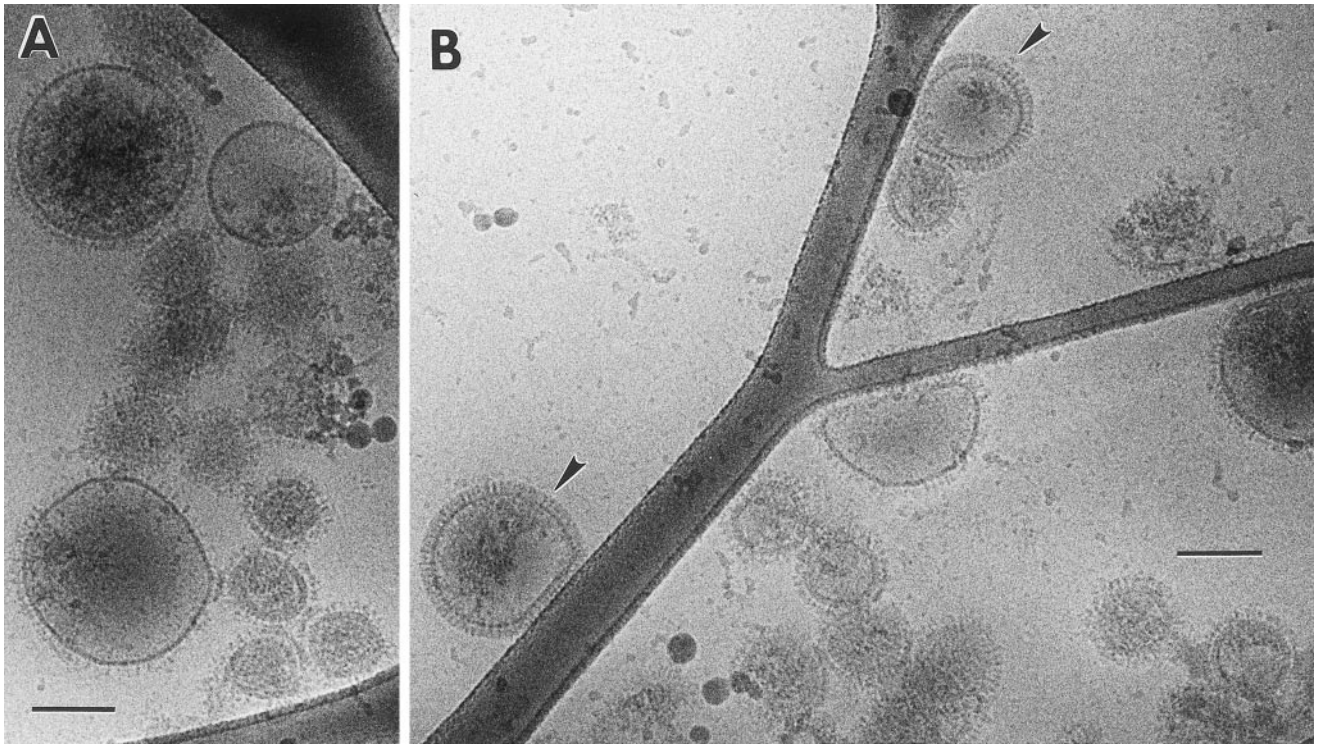

FIGURE 3 (*A*) Virions incubated for 30 min at pH 4.9. Note that most of the spike layers have become disorganized and resemble the virions incubated at pH 4.9 for longer times (Fig. 2, *D* and *E*). (*B*) Same conditions. Note that two virions (indicated by *arrowheads*) still have organized spike layers, with distinct and well-defined spikes, resembling virions at pH 7.4 (Fig. 2 *A*). Scale bars = 100 nm.

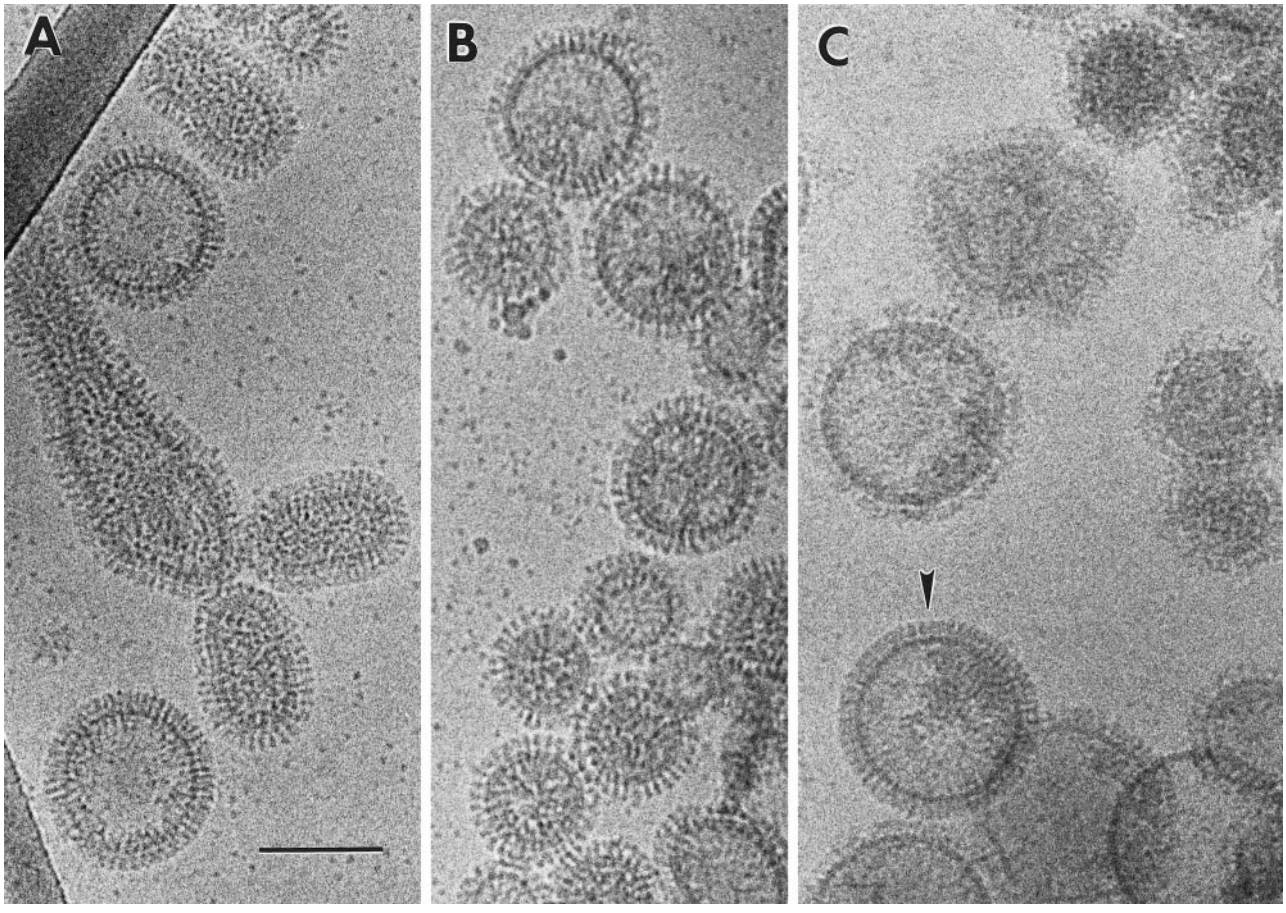

FIGURE 4 Higher magnification views of virions incubated at pH 7.4 (*A*), for 10 min at pH 4.9 (*B*), and for 68 min at pH 4.9 (*C*). The image in *C* is a magnified field of Fig. 2 *C*. The arrowhead indicates a virion that retains an organized spike layer, which is extremely rare under these conditions (see text). This is included to permit a side-by-side comparison with the more typical virions directly above it and around it, with disorganized spike layers. Parts *A–C* are at the same magnification (scale bar = 100 nm).

influenza virus (F. P. Booy, unpublished observations). These results are summarized in Table 1.

We performed CD studies on purified BHA because the morphological changes induced by low pH are thought to involve large changes in the secondary structure of individual segments of the protein (based on the BHA and TBHA2 crystal structures). It has already been reported that the total content of α-helix and β-sheet of BHA does not change significantly upon acidification (Ruigrok et al., 1988; Bullough et al., 1994), but these measurements were made well after viral inactivation was complete (Stegmann et al., 1990), and they could have missed transient intermediates, giving measurably different CD spectra. However, we observed essentially no change in θ_{222} for up to 76 min after acidification (data not shown). Korte et al. (1997) measured the CD signal at 283 nm, which reflects predominantly the three-dimensional arrangement and flexibility of Trp and Phe groups, rather than the proportion of different secondary structure. They observed a slow change in CD signal in Japan, X-31, and PR8 that appeared to correlate with the inactivation of intact virus under the same conditions.

TABLE 1 Morphological changes in virions as a function of time at pH 4.9 and 30°C

Condition	Tubular virions ($R > 2$)	Tubular virions ($R > 10$)	Blebs or membrane discontinuities	Sample size
pH 7.4	10%	1%	0.3%	399
pH 4.9, 2 min	1.4%	0.3%	0%	660
pH 4.9, 10 min	0.2%	0.05%	3%	2190
pH 4.9, 68 min	0%	0%	>20%	1201

R, Ratio of shortest to longest diameter.
At 60–68 min, most virions were in very large aggregates, and it was impossible to image the entire periphery of all of the virions. Thus many more than 20% of the virions may have had blebs or discontinuities.

DISCUSSION

Biochemical and crystallographic studies suggest that the influenza HA is likely to rearrange and form an extended triple-stranded coiled coil upon exposure to low pH (Carr and Kim, 1993; Bullough et al., 1994; Chen et al., 1995). The questions addressed in this investigation are whether this rearrangement occurs in intact viral HA and whether it represents the fusogenic or the inactivated state of HA. To put the results

in context, it important to examine models of the influenza HA derived from the crystallographic data at neutral (BHA) and low pH (TBHA2), and the implications of the structural rearrangements necessary for coiled-coil formation.

In Fig. 5, the crystal structure of BHA is shown on the left (at neutral pH; Wilson et al., 1981), with the helix-loop-helix region of HA2 highlighted to indicate those segments that ultimately form the coiled coil in TBHA2 (at low pH; Bullough et al., 1994), which is shown on the right of the figure. These are to be compared with a hybrid BHA/TBHA2 model in the center of Fig. 5. This hybrid model was constructed using the neutral pH base of BHA, substituting residues 38–76 (HA2) of TBHA2 for the corresponding residues in BHA and tilting the HA1 headgroups away from the three-fold axis by the rotation of a single bond in residue 20 to eliminate overlaps between HA1 and HA2. It assumes that the transmembrane segments of HA remain anchored to the viral envelope, the C-terminus of HA2 is not free to move because there is an envelope anchor (unlike for TBHA2), the HA-1 domain structure is not pH sensitive, and the coiled-coil stalk is perpendicular to the membrane surface. This extrapolation from the crystallographic data is intended to represent the most conservative possible rearrangement that permits the triple-stranded coiled coil of TBHA2 to emerge at low pH from the neutral pH form of BHA. In fact, the folding of the base of TBHA2, forming the small α-helix beyond residue 105 (see *right side* of Fig. 5), may not arise in viral HA.

These crystal structures show that the formation of a triple-stranded coiled coil by the HA2 segments has two significant consequences for relationships between the HA1 segments. First, residues 55–76 comprising the nonhelical (*yellow*) loop must traverse and separate the three HA1:HA1 interfaces present in the HA trimer to extend the coiled coil to involve residues 76–105. Second, once formed, the size of the coiled coil in cross section prevents reformation of the HA1:HA1 interfaces. These interfaces are relatively small (1350 $Å^2$) and not particularly hydrophobic, and there is no regular hydrogen bond array that traverses the interface. Thus little energy would be required to separate these domains. This model is consistent with recent studies, suggesting that elimination of HA1 permits EBHA2 (*Escherichia coli* expressed residues 38–175 of HA2) to form the stable coiled-coil structure at neutral pH (Chen et al., 1995) and that separation of the HA1 globular heads may be a trigger for coiled-coil assembly (Steinhauer et al., 1996). It is of interest to note that there are two Arg residues buried in the HA1-HA1 interface which, if charged, are stabilized only by carbonyl oxygens. The proximity of Arg^{220} and Arg^{229} raises the possibility that this pair is incompletely

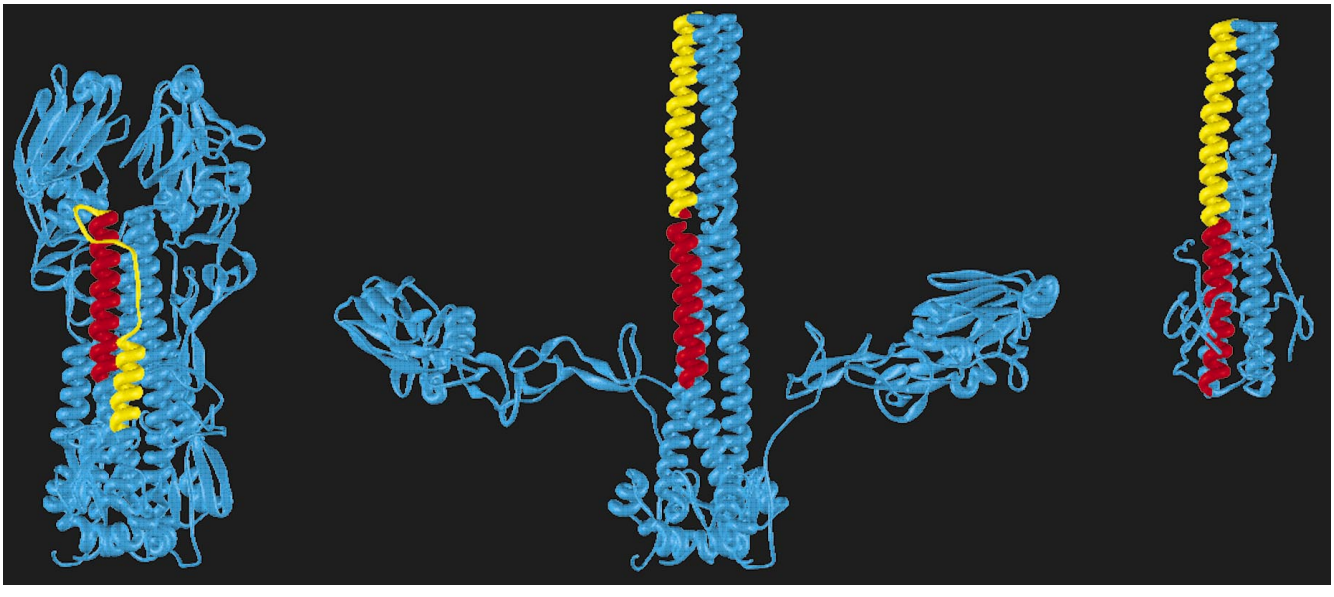

FIGURE 5 Model for the coiled-coil state of HA spikes. The intent of this model is to show the minimum rearrangements in BHA that are necessary to accommodate the helical coiled-coil of TBHA2. (*Left*) The neutral pH form of BHA (1HMG crystal structure; Wilson et al., 1981). The viral membrane is at the bottom of the figure, and the target membrane would be at the top. The HA1 chain nearest the viewer and the fusion peptides at the HA2 N-terminals (which would extend from the free ends of the *yellow helices*) have been removed for clarity. The yellow α-helix near the HA2 N-terminal is connected to the rest of the HA2 sequence (*red and blue regions*) by a loop region (also depicted in *yellow*). The bulbous domains at the top of the figure contain the sialic acid-binding domains of HA1. (*Right*) TBHA2 (the fragment of BHA crystallized at low pH; Bullough et al., 1994). In the TBHA2 structure, the loop region of HA2 becomes α-helical, and the red and yellow regions form a continuous α-helix. The long helix forms a coiled coil with the HA2 chains of the other two molecules in the trimer. The TBHA2 structure is aligned vertically with the BHA structure so that the bases of the "C" α-helical domains (shown in *red*) are at the same height in the figure. Note that TBHA2 represents only a fragment of the BHA molecule. (*Center*) Model for the coiled-coil form of HA spikes, based on the structures of BHA (Wilson et al., 1981) and TBHA2 (Bullough et al., 1994). The coiled coil was constructed by superimposing the base of the red "C" helices in TBHA2 (*right*) with the same region in BHA (*left*). These residues overlapped to high precision. Therefore, the coiled-coil domain of TBHA2 was grafted onto BHA, exchanging it for the same part of the BHA structure. The HA1 regions were then moved to resolve HA1-HA2 overlaps by rotating a single bond in residue 20 of the HA1 chain. The relative positions of the HA1 and HA2 chains were determined by the disulfide linkage of residues HA1–14 and HA2–137.

charged at neutral pH and that protonation at low pH could contribute to the dissociation of HA1 head groups.

If the globular HA1 domains are physically separated in the course of coiled-coil formation, we would expect the center of the structure to appear less electron dense, compared to BHA or native HA. We would also expect a significant loss of electron density at the base of HA2, below the disordered HA1 layer. The coiled-coil region itself would have a diameter of ~1.5 nm and would not generate much contrast in cryo-TEM. Moreover, the focal conditions used in Fig. 2 were chosen to highlight information on the length scale of the HA trimer width. Thus the conformational rearrangement illustrated in Fig. 5 (*center*) is consistent with the appearance of morphologically altered HA spikes in Figs. 2 *D* and 4.

The cryo-TEM results show that no major conformational change occurs in HA on the time scale of membrane fusion in the absence of a target membrane (within 10 min after acidification; Fig. 2 *C*). The conformational change that is consistent with the formation of the coiled coil develops only after ~30 min and is not seen to be complete until 60 min after acidification (Figs. 2 *D*, 2 *E*, and 3) i.e., during the time period when there is a significant degree of inactivation of the virions. These results are in qualitative agreement with observations of other influenza strains: Stegmann et al. (1987) and Puri et al. (1990) also observed disordered spike layers in X-47 or X-31 strains of influenza virus under conditions in which the virions were inactive. A/Japan/305/57, which inactivates much more slowly than the PR8 or X-47 strains, did not disorganize after 15 min at 37°C and low pH (Puri et al., 1990).

The appearance of an altered morphology on the same time scale as that of inactivation suggests that it represents the inactivated state of HA on isolated virions. Although the changes in morphology do not prove the type of structural change that occurs, we need only consider whether the morphological change does or does not represent the formation of the extended coiled coil. The former would show that the formation of the coiled coil on isolated virions results in inactivation, whereas the latter would show that the coiled coil is not involved in fusion, because it does not form on isolated virions on the time scale of either fusion or inactivation. We believe from the data presented that the morphological changes signaled the formation of the extended coiled coil.

The virions shown in Figs. 2–4 are what the liposomes would encounter in the fusion/inactivation experiment shown in Fig. 1. Although it is difficult to correlate the morphological changes observed to stages in the fusion process, because the cryo-TEM results were obtained with virions incubated in the absence of a target membrane, it is significant that no morphological changes were observed in HA spikes during the time scale of fusion. Thus the data suggest that the extended coiled-coil structure is not a precursor of HA-mediated fusion.

For the extended coiled-coil structure to be involved in fusion, one must assume that close apposition of the target membrane alters either the kinetics or the nature of the conformational change in HA at low pH. The extended coiled coil could be the end point of a sequence of conformational changes, where one or more intermediates are fusogenic. The kinetics of fusion do imply a multistep process (see reviews in Bentz, 1992, and Hernandez et al., 1996), and we propose the following scenario. Low pH releases the HA2 N-terminus from the interior of the trimer. The HA1:HA1 interfaces transiently stabilize the trimer against coiled-coil formation. In this intermediate, the exposed N-termini may function initially to aggregate individual HA molecules into a multimeric fusion site and/or interact with the viral bilayer. The opening of the HA1:HA1 interface permits the extended coiled coil to form. This opening would be facilitated by the close apposition of the target membrane, because fusion occurs well before the morphological change on isolated virions. The formation of the extended coiled-coil completes destabilization of the membranes, perhaps by drawing the aggregated HA closer together. This scenario is appealing, because it permits a simple coupling between the energy released by the formation of the coiled-coil and the energy needed to stabilize lipidic intermediates, which are likely to be quite energetic (Siegel, 1993).

In this regard, it is worth recalling that Shangguan et al. (1996a) found that target liposome membranes are sufficiently destabilized to allow leakage of aqueous contents (up to 10,000 MW dextran) simultaneously with the lipid mixing with influenza virions at low pH (see also Gunther-Ausborn et al., 1995). Such leakage suggests that one or more of the HA-fusion intermediates does not involve continuous bilayers. It is possible that the very extensive molecular rearrangements within HA during coiled-coil formation could facilitate the formation of such energetically unfavorable and leaky intermediates.

We thank Dr. John Silvius for providing us with fluorescent lipids. We are very grateful to Dr. Frank Booy for helpful advice and criticism of our cryo-TEM methods, for sharing his unpublished cryo-TEM observations of influenza virus with us, and for obtaining and analyzing the optical diffraction patterns of the micrographs in Fig. 2. DPS is also grateful to Ms. Nancy L. Reeder for technical assistance.

This work was supported in part by National Institutes of Health research grant GM31506.

REFERENCES

Alford, D., H. Ellens, and J. Bentz. 1994. Fusion of influenza virus with sialic acid-bearing target membranes. *Biochemistry.* 33:1977–1987.

Bartlett, G. R. 1959. Phosphorus assay in column chromatography. *J. Biol. Chem.* 234:466–468.

Bellare, J. R., H. T. Davis, L. E. Scriven, and Y. Talmon. 1988. Controlled environment vitrification system: an improved sample preparation technique. *J. Electron Microsc. Tech.* 10:87–111.

Bentz, J. 1992. Intermediates and kinetics of membrane fusion. *Biophys. J.* 63:448–459.

Bentz, J. 1993. Viral Fusion Mechanisms. CRC Press, Boca Raton, FL.

Bentz, J., H. Ellens, and D. Alford. 1990. An architecture for the fusion site of influenza hemagglutinin. *FEBS Lett.* 276:1–5.

Bentz, J., H. Ellens, and D. Alford. 1993. Architecture of the influenza hemagglutinin membrane fusion site. *In* Viral Fusion Mechanisms. J. Bentz, editor. CRC Press, Boca Raton, FL. 163–199.

Booy, F. P., R. W. H. Ruigrok, and E. F. J. van Bruggen. 1985. Electron microscopy of influenza virus. A comparison of negatively stained and ice-embedded particles. *J. Mol. Biol.* 184:667–676.

Brand, C. M., and J. J. Skehel. 1972. Crystalline antigen from the influenza virus envelope. *Nature New Biol.* 238:145–147.

Bullough, P. A., F. M. Hughson, J. J. Skehel, and D. C. Wiley. 1994. Structure of influenza haemagglutinin at the pH of membrane fusion. *Nature.* 371:37–43.

Carr, C. M., and P. S. Kim. 1993. A spring-loaded mechanism for the conformational change in influenza hemagglutinin. *Cell.* 73:823–832.

Carr, C. M., and P. S. Kim. 1994. Flu virus invasion: halfway there. *Science.* 266:234–236.

Chan, D. C., D. Fass, J. M. Berger, and P. S. Kim. 1997. Core structure of gp41 from the HIV envelope gylcoprotein. *Cell.* 89:263–273.

Chen, J., S. Wharton, W. Weissenhorn, L. Calder, F. Hughson, J. J. Skehel, and D. C. Wiley. 1995. A soluble domain of the membrane-anchoring chain of influenza virus hemagglutinin (HA2) folds in *Escherichia coli* into the low pH induced conformation. *Proc. Natl. Acad. Sci. USA.* 92:12205–12209.

Doms, R. W., A. Helenius, and J. White. 1985. Membrane fusion activity of the influenza virus hemagglutinin. *J. Biol. Chem.* 260:2973–2981.

Ellens, H., J. Bentz, D. Mason, F. Zhang, and J. M. White. 1990. Fusion of influenza hemagglutinin-expressing fibroblasts with glycophorin-bearing liposomes: role of hemagglutinin surface density. *Biochemistry.* 29:9697–9707.

Fujiyoshi, Y., N. P. Kume, K. Sakata, and S. B. Sato. 1994. Fine structure of influenza A virus observed by electron cryo-microscopy. *EMBO J.* 13:318–326.

Gething, M. J., R. W. Doms, D. York, and J. White. 1986. Studies on the mechanism of membrane fusion: site-specific mutagenesis of the hemagglutinin of influenza virus. *J. Cell Biol.* 102:11–23.

Godley, L., J. Pfeifer, D. Steinhauer, B. Ely, G. Shaw, R. Kaufmann, E. Suchanek, C. Pabo, J. J. Skehel, D. C. Wiley, and S. Wharton. 1992. Introduction of intersubunit disulfide bonds in the membrane-distal region of influenza hemagglutinin abolishes membrane fusion activity. *Cell.* 68:635–645.

Gunther-Ausborn, S., A. Praetor, and T. Stegmann. 1995. Inhibition of influenza-induced membrane fusion by lysophosphatylcholine. *J. Biol. Chem.* 270:29279–29285.

Hernandez, L. D., L. R. Hoffman, T. G. Wolfsberg, and J. M. White. 1996. Virus-cell and cell-cell fusion. *Annu. Rev. Cell Dev. Biol.* 12:627–661.

Korte, T., K. Ludwig, M. Krumbiegel, D. Zirwer, G. Damaschun, and A. Herrmann. 1997. Transient changes of the conformation of hemagglutinin of influenza virus at low pH detected by time-resolved circular dichroism spectroscopy. *J. Biol. Chem.* 272:9764–9770.

Nir, S., M. C. P. Lima, C. E. Larsen, J. Wilschut, D. Hoekstra, and N. Düzgünes. 1993. Kinetics and extent of virus-cell aggregation and fusion. *In* Viral Fusion Mechanisms. J. Bentz, editor. CRC Press, Boca Raton, FL. 437–452.

Puri, A., F. P. Booy, R. W. Doms, J. M. White, and R. Blumenthal. 1990. Conformational changes and fusion activity of influenza virus hemagglutinin of the H2 and H3 subtypes: effects of acid pretreatment. *J. Virol.* 64:3824–3932.

Ruigrok, R. W. H., A. Aitken, L. J. Calder, S. R. Martin, J. J. Skehel, S. A. Wharton, W. Weis, and D. C. Wiley. 1988. Studies on the structure of the influenza virus haemagglutinin at the pH of membrane fusion. *J. Gen. Virol.* 69:2785–2795.

Ruigrok, R. W. H., and E. A. Hewat. 1991. Comparison of negatively stained and frozen hydrated samples of influenza viruses A and B and of vesicular stomatitis virus. *Micron Microsc. Acta.* 22:423–434.

Ruigrok, R. W. H., E. A. Hewat, and R. H. Wade. 1992. Low pH deforms the influenza virus envelop. *J. Gen. Virol.* 73:995–998.

Ruigrok, R. W. H., N. G. Wrigley, L. J. Calder, S. Cusack, S. A. Wharton, E. B. Brown, and J. J. Skehel. 1986. Electron microscopy of the low pH structure of influenza virus haemagglutinin. *EMBO J.* 5:41–49.

Sato, S. B., K. Kawasaki, and S. I. Ohnishi. 1983. Hemolytic activity of influenza virus hemagglutinin glycoproteins activated in mildly acidic environments. *Proc. Natl. Acad. Sci. USA.* 80:3153–3157.

Shangguan, T. 1995. Molecular mechanism of influenza hemagglutinin mediated fusion. Ph.D. dissertation. Drexel University, Philadelphia.

Shangguan, T., D. Alford, and J. Bentz. 1996a. Influenza virus-liposomes lipid mixing is leaky and largely insensitive to the material properties of the target membrane. *Biochemistry.* 35:4956–4965.

Shangguan, T., D. Siegel, J. Lear, P. Axelsen, D. Alford, and J. Bentz. 1996b. Correlation of influenza virus fusion and inactivation with conformational changes in hemagglutinin. *Biophys. J.* 70:A439.

Siegel, D. P. 1993. Energetics of intermediates in membrane fusion: comparison of stalk and inverted micellar intermediate mechanisms. *Biophys. J.* 65:2124–2140.

Siegel, D. P., W. J. Green, and Y. Talmon. 1994. The mechanism of lamellar-to-inverted hexagonal phase transitions: a study using temperature-jump cryo-electron microscopy. *Biophs. J.* 66:402–414.

Silvius, J. R., R. Leventis, P. M. Brown, and M. Zuckermann. 1987. Novel fluorescent phospholipids for assays of lipid mixing between membranes. *Biochemistry.* 26:4279–4287

Skehel, J. J., P. M. Bayley, E. B. Brown, S. R. Martin, M. D. Waterfield, J. M. White, I. A. Wilson, and D. C. Wiley. 1982. Changes in the conformation of influenza virus hemagglutinin at the pH optimum of virus-mediated membrane fusion. *Proc. Natl. Acad. Sci. USA.* 79:968–972.

Stegmann, T., F. P. Booy, and J. Wilschut. 1987. Effects of low pH on influenza virus. Activation and inactivation of the membrane fusion capacity of the hemagglutinin. *J. Biol. Chem.* 262:17744–17749.

Stegmann, T., J. M. Delfino, F. M. Richards, and A. Helenius. 1991. The HA2 subunit of influenza hemagglutinin inserts into the target membrane prior to fusion. *J. Biol. Chem.* 266:18404–18410.

Stegmann, T., and A. Helenius. 1993. Influenza virus fusion: from models toward a mechanism. *In* Viral Fusion Mechanisms. J. Bentz, editor. CRC Press, Boca Raton, FL. 89–113.

Stegmann, T., S. Nir, and J. Wilschut. 1989. Membrane fusion activity of influenza virus: effects of gangliosides and negatively charged phospholipids in target liposomes. *Biochemistry.* 28:1698–1704.

Stegmann, T., J. M. White, and A. Helenius. 1990. Intermediates in influenza induced membrane fusion. *EMBO J.* 13:4231–4241.

Steinhauer, D. A., J. Martin, Y. P. Lin, S. A. Wharton, M. B. A. Oldstone, J. J. Skehel, and D. C. Wiley. 1996. Studies using double mutants of the conformational transitions in influenza hemagglutinin required for its membrane fusion activity. *Proc. Natl. Acad. Sci. USA.* 93:12873–12878.

Szoka, F. C., and D. Papahadjopoulos. 1978. Procedure for preparation of liposomes with large internal aqueous space and high capture by reverse phase evaporation. *Proc. Natl. Acad. Sci. USA.* 75:4194–4198.

Weber, T., G. Paesold, C. Galli, R. Mischler, G. Semenza, and J. Brunner. 1994. Evidence for H^+-induced insertion of influenza hemagglutinin HA2 N-terminal segment into viral membrane. *J. Biol. Chem.* 269: 18353–18358.

Weis, W. I., S. C. Cusack, J. H. Brown, R. S. Daniels, J. J. Skehel, and D. C. Wiley. 1990. The structure of a membrane fusion mutant of the influenza virus haemagglutinin. *EMBO J.* 9:17–24.

Weissenhorn, W., A. Dessen, S. C. Harrison, J. J. Skehel, and D. C. Wiley. 1997. Atomic structure of ectodomain from HIV-1 gp41. *Nature.* 371: 37–43.

Wharton, S. A., L. J. Calder, R. W. H. Ruigrok, J. J. Skehel, D. A. Steinhauer, and D. C. Wiley. 1995. Electron microscopy of antibody complexes of influenza virus haemagglutinin in the fusion pH conformation. *EMBO J.* 14:240–246.

White, J., and I. A. Wilson. 1987. Anti-peptide antibodies detect steps in a protein conformational change: low-pH activation of the influenza virus hemagglutinin. *J. Cell Biol.* 105:2887–2896.

White, J. M., J. Kartenbeck, and A. Helenius. 1982. Membrane fusion activity of influenza virus. *EMBO J.* 1:217–222.

Wild, C., J. W. Dubay, T. Greenwell, Jr., T. Baird, T. G. Oas, C. McDanal, E. Hunter, and T. Matthews. 1994. Propensity for a leucine zipper-like domain of human immunodeficiency virus type 1 gp41 to form oligomers correlates with a role in virus-induced fusion rather than assembly of the glycoprotein complex. *Proc. Natl. Acad. Sci. USA.* 91: 12676–12680.

Wiley, D. C., and J. J. Skehel. 1987. The structure and function of the hemagglutinin membrane glycoprotein of influenza virus. *Annu. Rev. Biochem.* 56:365–394.

Wilson, I. A., J. J. Skehel, and D. C. Wiley. 1981. Structure of the haemagglutinin membrane glycoprotein of influenza virus at 3 Å resolution. *Nature.* 289:366–373.

Yu, Y. G., D. S. King, and Y-K. Shin. 1994. Insertion of a coiled-coil peptide from influenza virus hemagglutinin into membranes. *Science.* 266:274–276.